

Optical absorption and activated transport in polaronic systems

G. Schubert,¹ G. Wellein,² A. Weiße,³ and H. Fehske¹

¹*Institut für Physik, Ernst Moritz Arndt Universität Greifswald, 17487 Greifswald, Germany*

²*Regionales Rechenzentrum Erlangen, Universität Erlangen, 91058 Erlangen, Germany*

³*School of Physics, The University of New South Wales, Sydney, NSW 2052, Australia*

(Dated: December 2, 2024)

We present exact results for the optical response in the one-dimensional Holstein model. In particular, by means of a refined kernel polynomial method, we calculate the ac and dc electrical conductivities at finite temperatures for the whole parameter range of electron phonon interaction. We analyze the deviations from the results of standard small polaron theory in the intermediate coupling regime and discuss non-adiabaticity effects in detail.

PACS numbers: 71.38.-k, 71.38.Ht, 74.25.Fy

The investigation of transport properties has been playing a central role in condensed matter physics for a long time. In recent years optical spectroscopy, for example, has contributed a lot to unravel the complex physics of highly correlated many-body systems, such as the one-dimensional (1d) MX chains,¹ the quasi-2d high-temperature superconducting cuprates,² or the 3d colossal magneto-resistive manganites.³ That way, optical measurements proved the importance of electron-phonon (EP) interactions in all these materials and, in particular, corroborated polaronic scenarios for modeling their electronic transport properties at least at high temperatures.^{4,5,6}

Polarons are quasi-particles composed of an electron and the surrounding ions which in a polar solid, provided the electron lattice interaction is sufficiently strong, are displaced from their equilibrium positions due to the presence of the electron. This bootstrap relation between electron and lattice displacement makes the particle heavy, because it has to drag with it the potential well of the phonons. Polaron motion is largely understood and has been worked out theoretically in two important limits. In the first case the electronic bandwidth is large and there is a only a slight change in the particle's effective mass due to the EP coupling. These quasi-particles are called large polarons or Fröhlich polarons. In the second case it is assumed that the bandwidth is small, whereas the EP interaction is strong and short-ranged. Now polaronic effects trap the electron at a certain lattice site and the size of the quasi-particle becomes comparable to the inter-atomic lattice spacing. Thermal activated hopping will necessarily be the dominant transport process of such small or Holstein-type polarons. Although there are experimental systems with clear large and small polaron characteristics, most of the above-mentioned novel materials belong to the transition region between these two limiting cases. Here the relevant energy scales are not well-separated and perturbative approaches cannot describe the complicated transport mechanisms adequately.

A recent non-perturbative dynamical mean-field study of the Holstein model in infinite dimensions⁷ reports quantitative discrepancies of the temperature dependence of the resistivity from standard polaron formulas,

but the dynamical mean-field approach inherently does not account for vertex corrections to the conductivity and for longer ranged hopping processes induced by the EP interaction. On the other hand, exact numerical investigations of the Holstein model provided quite a number of reliable data for the zero-temperature optical conductivity in the 1d and 2d (extended) Holstein models.^{8,9}

Motivated by this situation, in the present work, we make use of the Kernel Polynomial Method (KPM),^{10,11} a refined numerical Chebyshev expansion technique which enables us to compute both the dc and ac hopping conductivities at finite temperatures without any serious approximation.

Our starting point is the 1d tight-binding Holstein Hamiltonian,¹²

$$H = -t \sum_{\langle i,j \rangle} c_i^\dagger c_j - \sqrt{\varepsilon_p \omega_0} \sum_i (b_i^\dagger + b_i) n_i + \hbar \omega_0 \sum_i b_i^\dagger b_i, \quad (1)$$

describing a single electron coupled locally to a dispersion-less optical phonon mode, where c_i^\dagger (b_i^\dagger) denotes the corresponding fermionic (bosonic) creation operator, and $n_i = c_i^\dagger c_i$. Setting $\hbar = 1$ and measuring all energies in units of the nearest-neighbor hopping integral t , the physics of the model is determined by the dimensionless EP coupling constants

$$\lambda = \varepsilon_p / 2t \quad \text{and} \quad g^2 = \varepsilon_p / \omega_0 \quad (2)$$

in the adiabatic ($\omega_0/t \ll 1$) and anti-adiabatic ($\omega_0/t \gg 1$) regimes, respectively. In 1d the crossover from large to small polaron behavior takes place at $\lambda \simeq 1$ ($g^2 \simeq 1$) in the former (latter) case.^{13,14} Whether large polarons form in the Holstein model for $d > 1$ is still under debate.^{15,16,17}

Addressing the linear response of our system to an external (longitudinal) electric field we consider the Kubo formula for the electrical conductivity at finite temperatures, which is¹⁸

$$\text{Re } \sigma(\omega) = \pi \sum_{m,n}^{\infty} \frac{e^{-\beta E_n} - e^{-\beta E_m}}{Z L \omega} |\langle n | j | m \rangle|^2 \delta(\omega - \omega_{mn}). \quad (3)$$

Here $Z = \sum_n^\infty e^{-\beta E_n}$ is the partition function and $\beta = (k_B T)^{-1}$ denotes the inverse temperature. Since the Holstein Hamiltonian (1) involves bosonic degrees of freedom, the Hilbert space even of a finite L -site system has infinite dimension. In practice, however, the contribution of highly excited phonon states is negligible at the relevant temperatures, and the system is well approximated by a truncated phonon space with at most $M(\lambda, g, \omega_0; T)$ phonons.¹⁹ Then $|n\rangle$ and $|m\rangle$ are the eigenstates of H within our truncated D -dimensional Hilbert space, E_n and E_m are the corresponding eigenvalues, and $\omega_{mn} = E_m - E_n$. In Eq. (3) the current operator has the standard hopping form, $\hat{j} = i e t \sum_i (c_i^\dagger c_{i+1} - c_{i+1}^\dagger c_i)$, and connects states with different parity. Thus, assuming that the ground state is non-degenerate, the expectation value $\langle 0 | \hat{j} | 0 \rangle$ vanishes in the absence of an external electric field. The limit $\omega \rightarrow 0$ of (3) yields the dc conductivity, whereas the optical absorption is given by the finite frequency data. For small polarons both results are interesting and have been evaluated analytically at an early stage.²⁰ At $T = 0$, the regular part of the optical conductivity, $\sigma^{\text{reg}}(\omega) = \frac{\pi}{L} \sum_{n>0} \omega_{n0}^{-1} |\langle n | \hat{j} | 0 \rangle|^2 \delta(\omega - \omega_{n0})$, was calculated for finite 1d and 2d lattices with periodic boundary conditions (PBC) and the entire parameter range of the Holstein model, using a combination of the Lanczos algorithm and the KPM.⁸

At finite temperatures, a similar straight-forward expansion of the conductivity is spoiled by the presence of the Boltzmann factors and the contribution of all matrix elements between eigenstates of the system. Instead, it turns out that a new generalised KPM scheme^{11,21} can be based upon a current operator density

$$j(x, y) = \sum_{m,n} |\langle n | \hat{j} | m \rangle|^2 \delta(x - E_n) \delta(y - E_m). \quad (4)$$

Being a function of two variables, $j(x, y)$ can be expanded by a two-dimensional KPM,

$$\tilde{j}(x, y) = \sum_{k,l=0}^{N-1} \frac{\mu_{kl} w_{kl} g_k^J g_l^J T_k(x) T_l(y)}{\pi^2 \sqrt{(1-x^2)(1-y^2)}}, \quad (5)$$

where the tilde refers to a rescaling of energy ($H \rightarrow \tilde{H}$), that maps the spectrum of H into the domain $[-1, 1]$ of the Chebyshev polynomials of first kind $T_k(x)$. The finite order N of the expansion leads to Gibbs oscillations which can be damped by introducing appropriate damping factors. Here we use g_n^J derived from the Jackson kernel.^{10,22} The core of the numerical work is the iterative calculation of the moments $\mu_{kl} = \text{Tr}(T_k(\tilde{H}) \hat{j} T_l(\tilde{H}) \hat{j})$, where the trace can be replaced by an average over a relatively small number of random vectors $|r\rangle$.²³ Finally, the factors $1/w_{kl} = (2 - \delta_{k0})(2 - \delta_{l0})$ account for the correct normalisation. Given the operator density $j(x, y)$ we find

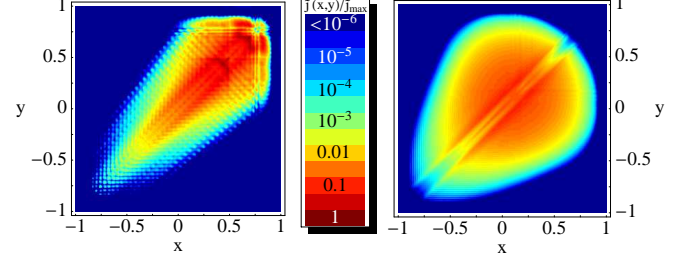


FIG. 1: (Color online) Renormalized current operator density $\tilde{j}(x, y)$ used in the 2d KPM. Data obtained for the 1d Holstein model with $\lambda = 0.2$ (left panel) and $\lambda = 2.0$ (right panel) at $\omega_0/t = 0.4$ ($L = 6, M = 50$; PBC).

the optical conductivity by integration

$$\text{Re } \sigma(\omega) = \frac{\pi}{Z L \omega} \int_{-\infty}^{\infty} j(y + \omega, y) [e^{-\beta y} - e^{-\beta(y+\omega)}] dy. \quad (6)$$

The partition function $Z = \int_{-\infty}^{\infty} \rho(E) \exp(-\beta E)$ is easily obtained by integrating over the density of states $\rho(E) = \sum_{n=0}^{D-1} \delta(E - E_n)$, which can be expanded in parallel to $\tilde{j}(x, y)$. Note the main advantage of this approach: The current operator density that enters the conductivity is the same for all temperatures, i.e., it needs to be expanded only once. Figure 1 exemplifies the different form of $\tilde{j}(x, y)$ in the weak and strong EP coupling regimes.

At very low temperatures, the numerical evaluation of expression (6) requires some caution, since the Boltzmann factors heavily amplify small numerical errors in $j(y + \omega, y)$. We can avoid these problems, occurring mainly at the lower bound of the spectrum, by treating the contributions of the ground state and some of the lowest excitations separately. This is illustrated in Fig. 2. We

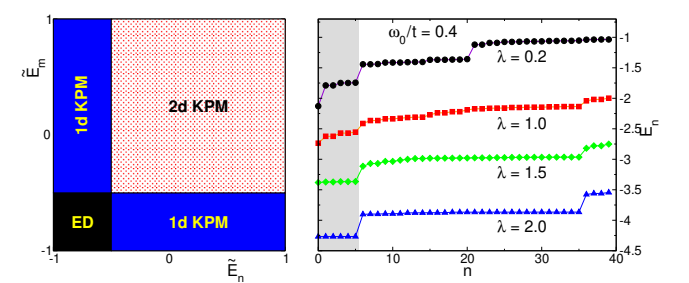


FIG. 2: (Color online) Schematic setup for the calculation of the finite-temperature optical conductivity (left panel). Lowest eigenvalues of the Holstein Hamiltonian for $L = 6, M = 25$, and PBC (right panel). The shaded area marks the six lowest eigenvalues to be separated from the rest of the spectrum.

split the optical conductivity into three parts,

$$\text{Re } \sigma(\omega) = \text{Re } \sigma_{\text{ED}}(\omega) + \text{Re } \sigma_{\text{KPM}}^{\text{1d}}(\omega) + \text{Re } \sigma_{\text{KPM}}^{\text{2d}}(\omega), \quad (7)$$

where the first contribution describes the transitions (matrix elements) between the S separated eigenstates, the second part those between the separated states and the rest of the spectrum, which can be expressed as standard 1d KPM expansions, and finally the transitions within the remaining $D - S$ states of the spectrum, handled by a 2d expansion. Using the projection operator $P = 1 - \sum_{s=0}^{S-1} |s\rangle\langle s|$, the moments for the contributions $\text{Re } \sigma_{\text{1d}}(\omega)$ read $\mu_k^n = \langle n | \hat{J} P T_k(\tilde{H}) P \hat{J} | n \rangle$. Of course, the number of states one has to separate depends on the physical situation. The right panel of Fig. 2 gives the lowest eigenvalues of the Holstein model at various coupling strengths. In the strong-coupling regime ($\lambda \gg 1$) states belonging to the lowest small polaron band have almost the same energy as the ground state and therefore should be treated separately (cf. the curves for $\lambda = 1.5$ and 2). Obviously the situation is far less dramatic at weak EP couplings.

We now apply our numerical scheme to the calculation of the optical absorption in the 1d Holstein model. The results for $\text{Re } \sigma(\omega)$ are important for relating theory and experiment. Figure 3 shows data obtained at $\omega_0 = 0.4t$ and $\lambda = 2$, i.e., at rather large EP coupling, but not in the extreme small-polaron limit. Hence, the maximum of the low-temperature optical response is located somewhat below $2\varepsilon_p/t$, being the value for small polarons at $T = 0$. At the same time, the line-shape is more asymmetric than in standard polaron theory, with a weaker decay at the high-energy side, which fits even better the experimental behavior observed in polaronic materials such as TiO_2 .²⁴ Clearly, coherent transport, which for large EP couplings is related to diagonal (zero-phonon) transitions within the lowest extremely narrow polaron band, will be strongly suppressed at finite temperatures. For instance, the amplitude of the current matrix elements between the degenerate states with momentum $K = \pm\pi/3$ ($K = 0, \pm\pi/3, \pm 2\pi/3$, and π are the allowed wave numbers of a 6-site system with PBC) is of the order of 10^{-7} only. Whereas phase coherence is maintained during a diagonal transition, the particle loses its phase coherence if its motion is triggered by (multi-) phonon absorption and emission processes. These so-called non-diagonal transitions which, of course, can take place also with zero energy transfer, become more and more important as the temperature increases. Now the main transport mechanism is thermal activated hopping, where each hop becomes a statistically independent event. In the small polaron limit, where the polaronic sub-bands are roughly separated by the bare phonon frequency (cf. Fig. 2, right panel), this happens for $k_B T \gtrsim \omega_0$. Let us consider the activated regime in more detail: With increasing temperatures we observe a substantial spectral weight transfer to lower frequencies, and an increase of the zero-energy transition probabil-

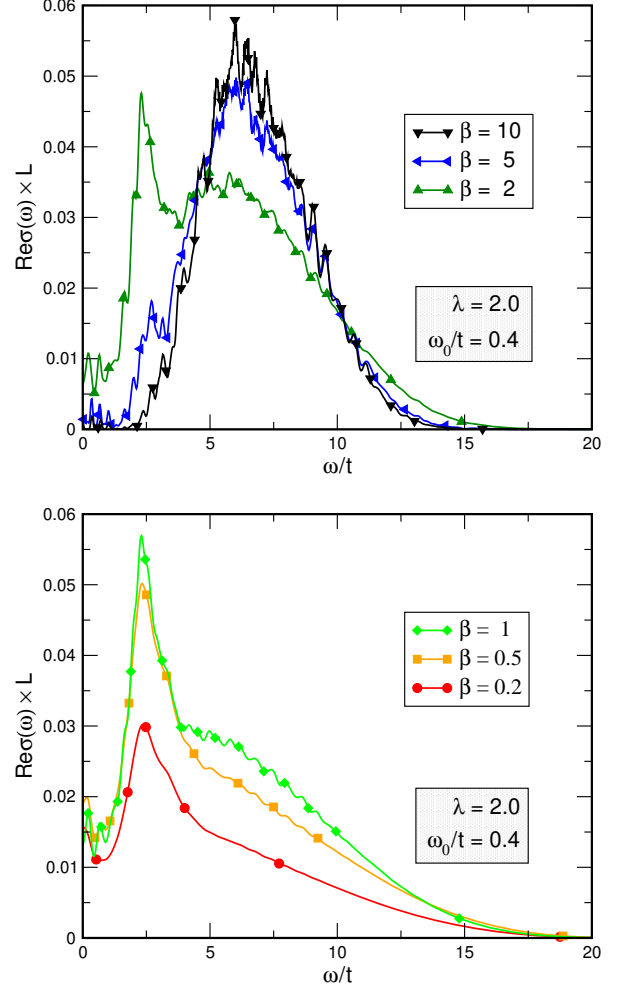


FIG. 3: (Color online) Optical absorption by small polarons at finite temperatures in the adiabatic regime.

ity in accordance with previous results.²⁵ In addition, we find a strong resonance in the absorption spectra at about $\omega \sim 2t$, which can be easily understood using a configurational coordinate picture. Placing a homogeneous lattice distortion u at L_u consecutive sites by applying the unitary transformation $S^\dagger(u) = \prod_{i=1}^{L_u} S_i^\dagger(u) = \prod_{i=1}^{L_u} \exp[u(b_i^\dagger - b_i)]$, the transformed Holstein Hamiltonian takes the form $\tilde{H} = \langle 0 | S^\dagger(u) H S(u) | 0 \rangle_{\text{ph}} = -t \sum_{\langle i,j \rangle} c_i^\dagger c_j - 2\sqrt{\varepsilon_p \omega_0} u \sum_i^{L_u} n_i + \omega_0 u^2 L_u$. In the adiabatic strong-EP-coupling regime, the ground state can be approximated as an electron localized at a certain single site with the lattice being in a shifted oscillator state ($L_u = 1$). That is, $|\Psi_0\rangle = |1\rangle_{\text{el}} \otimes S_1^\dagger(g) |0\rangle_{\text{ph}}$ and $E_0 = -\varepsilon_p$, in accordance with the Lang-Firsov approximation. Now let us consider excitation from this ground-state, where the lattice distortion spreads over two neighboring sites ($L_u = 2$) and the electron is in a symmetric or antisymmetric linear combination of $|1\rangle_{\text{el}}$ and $|2\rangle_{\text{el}}$, i.e., the particle is mainly located at sites 1 and 2 but delocalized between these sites. We then

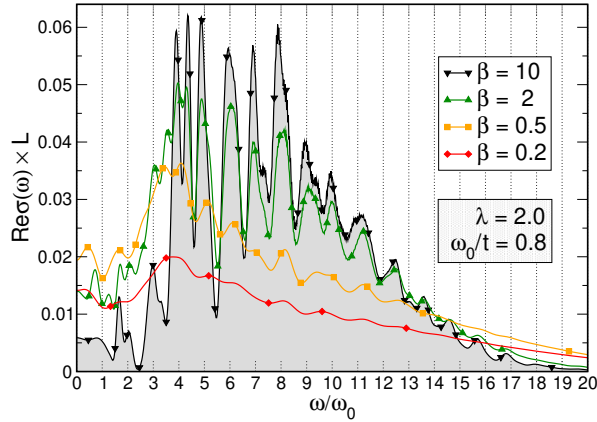


FIG. 4: (Color online) Optical absorption by small polarons at finite temperatures in the non-adiabatic regime. Note that now the abscissa is scaled with respect to the phonon frequency.

find $|\Psi_{1,\pm}\rangle = (|1\rangle_{el} \pm |2\rangle_{el}) \otimes S_2^\dagger(g/2)S_1^\dagger(g/2)|0\rangle_{ph}$ and $E_{1,\pm} = \mp t - \varepsilon_p/2$. Whereas the (potential) energy related to the displacement field is reduced to $-\varepsilon_p/L_u$, the kinetic energy comes into play since hopping processes between 1 and 2 are allowed. The current operator \hat{j} connects these different-parity states with perfect overlap $|\langle\Psi_{1,+}|\hat{j}|\Psi_{1,-}\rangle| = (et)^2$, giving rise to a strong signal in the optical absorption. Note that the excitation energy $\omega_{1,-1,+} = 2t$ is independent of ε_p . In order to activate these transitions thermally, the electron has to overcome the “adiabatic” barrier $\Delta = E_{1+} - E_0 = \varepsilon_p/2 - t$. A finite phonon frequency will relax this condition. From Fig. 3, we find the signature to occur above $k_B T \gtrsim 0.5t$. Of course, one could also extend this scenario to excitations where the electron is delocalized over more than two distorted lattice sites, but for the present parameters the signature of these weakly bound states would be rather small.

Entering the non-adiabatic regime of large phonon frequencies at fixed $\lambda = 2$, the pattern of sub-bands separated roughly by ω_0 becomes more pronounced, but is, of course, washed out at higher temperatures (see Fig. 4 for $\omega_0/t = 0.8$). In Fig. 4 the average number of phonons contained in the ground state ($\propto g^2$) is smaller ($g^2 = 5$) than in the previous case where $g^2 = 10$ ($\omega_0/t = 0.4$). This also concerns the activated region $\omega_0/t \lesssim k_B T \lesssim \Delta$ but for these parameters the simple adiabatic picture anticipated above breaks down anyway.

Now let us decrease the EP coupling strength at small phonon frequencies $\omega_0/t = 0.2$ keeping $g^2 = 10$ fixed. Results for the optical response in the vicinity of the large to small polaron crossover ($\lambda = 1$) are depicted in Fig. 5. Here the small polaron maximum has almost disappeared and the $2t$ -absorption feature can be activated at very low temperatures ($\Delta \rightarrow 0$ for the two-site model with $\lambda = 1$). The overall behavior of $\text{Re}\sigma(\omega)$ resembles that of polarons of intermediate size. At high temperatures these polarons will dissociate readily and

the transport properties are equivalent to those of electrons scattered by thermal phonons. Let us emphasize that many-polaron effects become increasingly important in the large-to-small polaron transition region.²⁶ As a result, polaron transport might be changed entirely compared to the one-particle picture discussed so far.

Before we consider the temperature dependence of the dc conductivity, it is useful to test the sum rules for the real part of the optical response. First we have the so-called *f*-sum rule,

$$S_{tot} := \int_{-\infty}^{\infty} \text{Re}\sigma(\omega)d\omega = \frac{\pi e^2}{L} E_{kin}, \quad (8)$$

which relates the ω -integrated $\text{Re}\sigma(\omega)$ to the kinetic energy $E_{kin} = -t \sum_{\langle i,j \rangle} \langle c_i^\dagger c_j \rangle$. Note that the $\omega = 0$ (Drude) contribution is included in (8). The second sumrule for $\text{Re}\sigma(\omega)$ is

$$\int_0^{\infty} \omega \text{Re}\sigma(\omega)d\omega = \frac{\pi e^2}{L} \langle j^2 \rangle_T. \quad (9)$$

Throughout our calculations Eq. (9) was fulfilled within numerical accuracy, where the thermal average $\langle j^2 \rangle_T$ was determined again using a 1d KPM. Exploiting sum rule (8) we get important information about finite-size effects.

Figure 6 compares E_{kin} and $S_{tot}L/\pi e^2$ obtained from our finite-cluster calculation. At weak EP couplings the kinetic energy is a strictly monotonic decreasing function of temperature and becomes strongly suppressed at high temperatures due to scattering of the electron by thermal phonons. Whereas the *f*-sum rule is almost perfectly fulfilled for smaller values of β , we found pronounced deviations at low temperatures which, without doubt, can be assigned to the finite size of our Holstein ring (cf. the L dependence of S_{tot} shown in the upper panel of Fig. 6, and also the discussion of the dc conductivity below). Clearly finite-size effects become important when the temperature is comparable to the energy gaps in the spectrum of H (see Fig. 2). At strong

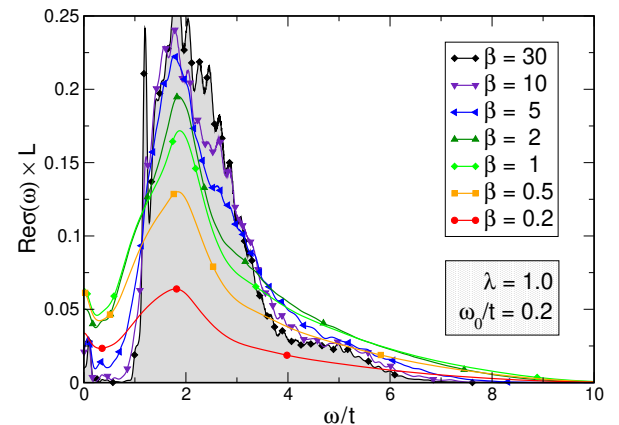


FIG. 5: (Color online) Optical absorption in the adiabatic intermediate EP-coupling regime (g^2 is the same as in Fig. 3).

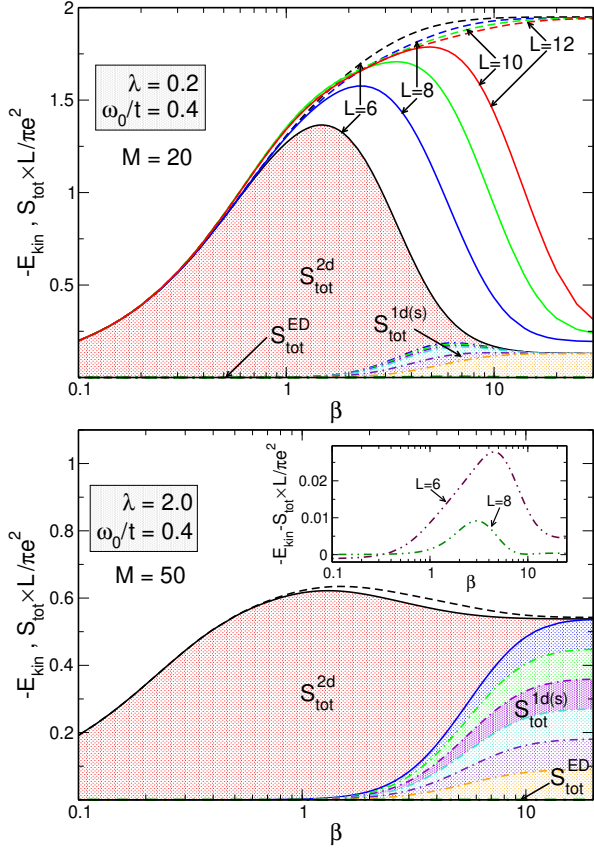


FIG. 6: (Color online) Conformance of the f -sum rule (8) in the weak (upper panel) and strong (lower panel) EP coupling regimes of the 1d Holstein model. Results for S_{tot} , partial S_{tot} 's and E_{kin} are given by solid, dot-dashed and dashed lines, respectively. For further explanation see text.

EP couplings the transport is hopping-dominated and the kinetic energy exhibits a maximum at a finite temperature that can be related to the thermal activation energy of polarons. Now, in view of the narrow small-polaron band (cf. Fig. 2), finite size gaps are small and the f -sum rule is fulfilled down to very low temperatures. Small deviations appear to vanish rapidly with increasing system size (see inset, lower panel of Fig. 6). In order to analyze the contributions of different transport processes to E_{kin} in some more detail, we have decomposed $S_{tot} = S_{tot}^{ED} + \sum_{s=0}^{S-1} S_{tot}^{1d(s)} + S_{tot}^{2d}$ in analogy to Eq. (7). Figure 6 shows that the coherent (intra-band) contribution ($\propto S_{tot}^{ED}$) is almost negligible at the temperatures considered. Inter-band transitions connecting eigenstates of the lowest polaron band to higher excited states (1d KPM) are the determining factor at low T . If the renormalised polaron bandwidth is small enough, all states in the band are equally populated, leading to pretty much the same values of $S_{tot}^{1d(s)}$. At high temperatures, of course, the transitions covered by the 2d KPM are predominant.

The dc conductivity is obtained by taking the limit

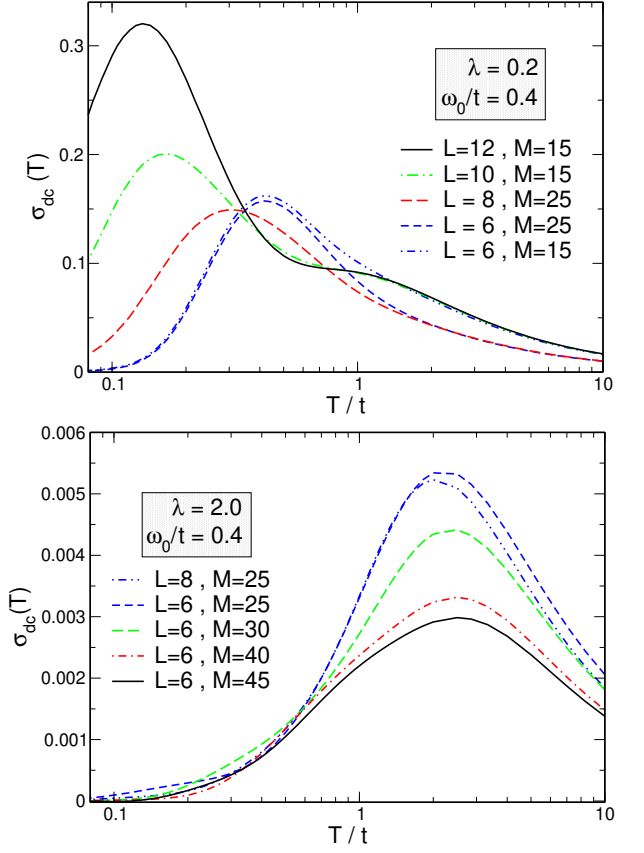


FIG. 7: (Color online) DC conductivity as a function of temperature at weak (upper panel) and strong (lower panel) EP coupling.

$\omega \rightarrow 0$ of (3), which with $\lim_{\omega \rightarrow 0} (1 - e^{-\beta\omega})/\omega = \beta$ yields

$$\text{Re } \sigma_{dc} = \frac{\pi\beta}{ZL} \sum_{n,m=0}^{D-1} e^{-\beta E_n} |\langle n | \hat{j} | m \rangle|^2 \delta(E_m - E_n). \quad (10)$$

Since we have $\langle 0 | \hat{j} | 0 \rangle = 0$ the conductivity is finite as $\omega \rightarrow 0$ and $\text{Re } \sigma_{dc}$ essentially counts the number of thermally accessible current carrying (degenerate) states. In the thermodynamic limit $\text{Re } \sigma_{dc}$ gives the charge stiffness D_c , [or the so-called Drude weight (at $T = 0$)].²⁷

The temperature dependence of the dc conductivity is illustrated in Fig. 7. Again the weak coupling results appear to have a rather strong finite-size dependence (note that $\text{Re } \sigma_{cd}$ depicted in Fig. 7 is an intensive quantity). When L increases a pronounced peak develops at low temperatures. This peak can be attributed to a normal “metallic-like” behavior. Since $\varepsilon_p > 0$ we expect that $\text{Re } \sigma(\omega \rightarrow 0)$ is finite for $T \rightarrow 0$ and $L \rightarrow \infty$. The shoulder observed for the 10 and 12 site systems at $T/t \gtrsim 1$ is obviously an artifact of our phonon Hilbert space truncation as can be seen by comparing the data obtained for $L = 6$ and different numbers of the phonon cut-off M . In the strong-EP-coupling polaronic regime, band-like transport becomes extensively suppressed (the Drude weight is exponentially small). Nevertheless quan-

tum zero-point phonon fluctuations cause polaron delocalization at $T = 0$. At higher temperatures incoherent polaron hopping transport manifests in the temperature dependence, leading to the well-known absorption maximum in $\text{Re } \sigma_{dc}(T)$ (cf. Fig. 7, lower panel). Since this signature is related to (rather local) polaron excitation processes the position of the maximum is almost independent of the system size.

To summarize, we have investigated the motion of a charge carrier in response to ac and dc external fields for strongly coupled electron-phonon systems. The combination of Lanczos diagonalization and the Kernel Polynomial Method has enabled us to calculate for the first time quasi-exactly the temperature dependence of the optical absorption spectra and the dc conductivity in the framework of the one-dimensional Holstein model. Finite-size effects were assessed and eliminated, e.g., on the basis of the f -sum rule. In the physically most interesting range

of intermediate coupling strengths and phonon frequencies, we find that the conductivity significantly deviates from the standard small-polaron results.

Acknowledgments

We are grateful to A. Alvermann, M. Hohenadler, and J. Loos for helpful discussions. This work was supported by the Deutsche Forschungsgemeinschaft through SPP1073, by KONWIHR and by the Australian Research Council. H. F. acknowledges the hospitality at the University of New South Wales sponsored by the Gordon Godfrey Bequest. Special thanks go to NIC Jülich and HLRN Berlin for generously granting access to their supercomputer facilities.

¹ A. R. Bishop and B. I. Swanson, Los Alamos Science **21**, 133 (1993); H. Fehske, M. Kinateder, G. Wellein, and A. R. Bishop, Phys. Rev. B **63**, 245121 (2001).

² E. Dagotto, Rev. Mod. Phys. **66**, 763 (1994); S. Tajima, Y. Fudamoto, T. Kakeshita, B. Gorshunov, V. Železní, K. M. Kojima, M. Dressel, and S. Uchida, Phys. Rev. B **71**, 094508 (2005).

³ S. Jin, T. H. Tiefel, M. McCormack, R. A. Fastnach, R. Ramesh, and L. H. Chen, Science **264**, 413 (1994); A. Weiße and H. Fehske, New J. Phys. **6**, 158 (2004).

⁴ D. Emin, Phys. Rev. B **48**, 13691 (1993).

⁵ A. S. Alexandrov and N. F. Mott, *Polarons and Bipolarons* (World Scientific, Singapore, 1995).

⁶ D. C. Worledge, L. Miéville, and T. H. Geballe, Phys. Rev. B **57**, 15267 (1998).

⁷ S. Fratini, F. de Pasquale and S. Ciuchi, Phys. Rev. B **63**, 153101 (2001); S. Fratini and S. Ciuchi, Phys. Rev. Lett. **91**, 256403 (2003).

⁸ H. Fehske, J. Loos, and G. Wellein, Z. Phys. B **104**, 619 (1997); G. Wellein and H. Fehske, Phys. Rev. B **58**, 6208 (1998); H. Fehske, J. Loos, and G. Wellein, Phys. Rev. B **61**, 8016 (2000).

⁹ C. Zhang, E. Jeckelmann, and S. R. White, Phys. Rev. B **60**, 14092 (1999).

¹⁰ R. N. Silver, H. Röder, A. F. Voter, and D. J. Kress, J. of Comp. Phys. **124**, 115 (1996).

¹¹ A. Weiße, G. Wellein, A. Alvermann, and H. Fehske (2005), URL <http://arXiv.org/abs/cond-mat/0504627>.

¹² T. Holstein, Ann. Phys. (N.Y.) **8**, 325 (1959); *ibid* **8**, 343 (1959).

¹³ G. Wellein and H. Fehske, Phys. Rev. B **56**, 4513 (1997).

¹⁴ M. Capone, W. Stephan, and M. Grilli, Phys. Rev. B **56**, 4484 (1997).

¹⁵ D. Emin, Phys. Rev. B **48**, 3973 (1986); V. V. Kabanov and O. Y. Mashtakov, Phys. Rev. B **47**, 6060 (1993).

¹⁶ H. Fehske, H. Röder, G. Wellein, and A. Mistriotis, Phys. Rev. B **51**, 16582 (1995); L.-C. Ku, S. A. Trugman, and J. Bonča, Phys. Rev. B **65**, 174306 (2002).

¹⁷ V. Cataudella, G. D. Filippis, and G. Iadonisi, Phys. Rev. B **60**, 153163 (1999); *ibid* **63**, 052406 (2001).

¹⁸ G. D. Mahan, *Many-Particle Physics* (Kluwer Academic/Plenum Publishers, New York, 2000).

¹⁹ B. Bäuml, G. Wellein, and H. Fehske, Phys. Rev. B **58**, 3663 (1998).

²⁰ I. G. Lang and Y. A. Firsov, Zh. Eksp. Teor. Fiz. **43**, 1843 (1962); Y. A. Firsov, *Polarons* (Izd. Nauka, Moscow, 1975); Y. A. Firsov, Semiconductors **29**, 515 (1995).

²¹ A. Weiße, Eur. Phys. J. B **40**, 125 (2004).

²² D. Jackson, Trans. Amer. Math. Soc. **13**, 491 (1912).

²³ D. A. Drabold and O. F. Sankey, Phys. Rev. Lett. **70**, 3631 (1993).

²⁴ E. K. Kudinov, D. N. Mirlin, and Y. A. Firsov, Fiz. Tverd. Tela **11**, 2789 (1969).

²⁵ E. L. Nagaev, Sov. Phys. Solid State **4**, 1611 (1963).

²⁶ M. Hohenadler, D. Neuber, W. von der Linden, G. Wellein, J. Loos, and H. Fehske (2004), accepted for publication in Phys. Rev. B, URL <http://arXiv.org/abs/cond-mat/0412010>.

²⁷ B. S. Shastry and B. Sutherland, Phys. Rev. Lett. **65**, 243 (1990); B. N. Narozhny, A. J. Millis, and N. Andrei, Phys. Rev. B **58**, R2921 (1998).